Toward On-Chip Unidirectional and Single-Mode Polymer Microlaser

Xue-Peng Zhan, Ying-Xin Xu, Huai-Liang Xu, Qiu-Lan Huang, Zhi-Shan Hou, Wei Fang, Qi-Dai Chen, and Hong-Bo Sun, *Member, IEEE*

***Abstract*—Optical microcavities have been paid enormous attentions as a basic integrated element in photonic devices including micromodulators, microfilters, and microsensors. In particular, the microcavities that can produce unidirectional and single-mode lasing emissions are greatly demanded to meet the challenge of integrating high-efficiency and high-sensitivity optical functional systems. Herein, a three-dimensional polymer microlaser composed of stacked circular-ring-shaped and spiral-ring-shaped microcavities is fabricated directly on a narrow bandpass filter substrate by the femtosecond laser processing technique. The on-chip polymer microlaser provides a room-temperature, low-threshold, unidirectional, and single-mode laser output, resulting from the coupling between the two stacked microcavities. The fabrication of the on-chip low-threshold polymer microlaser opens up a possibility toward the integration of a variety of polymer microcavities for organic optoelectronic devices.**

***Index Terms*—Laser processing, microresonators, optical polymer, single mode, unidirectional.**

I. Introduction

OPTICAL microcavities that hold the major advantages of small volume and high-quality (Q) factor have been considered as important platforms for fundamental investigations of light-matter interaction such as cavity opto-mechanics [1]–[3], cavity quantum electrodynamics [4], [5] and quantum information [6], [7]. They are also serving as elements of integrated photonic devices for a broad spectrum of applications including micro-modulators [8], [9], micro-filters [10], [11], microsensors [12], [13] and so forth. Specially, the microcavities based on Whispering-Gallery-Modes (WGMs) have been extensively investigated in recent years because of their ultra-low loss, ultra-high Q factor and ultra-high sensitivity to surrounding materials [14]–[18]. However, owing to the total internal reflection of light at the rotational symmetrical interface [15], the WGMs microcavities exhibit isotropic emissions in both the near and far fields, leading to less efficiency for applications, for example, in producing lasing emissions.

Recently, deformed microlasers (DMs) that can produce highly directional emissions by breaking the rotational symmetry of the WGMs microcavities have attracted a lot of interest [19]–[27]. Among various types of DMs, spiral-shaped microlaser has been paid special attention owing to its ability of producing unidirectional radiation without significant spoiling of the Q factor [26], [27]. On the other hand, when compared with multi-mode microlasers, single-mode ones are more desirable in many applications [28]–[31]. Therefore, several efforts have been made to design special microcavity structures for producing both unidirectional and single-mode radiation. For instance, Huang *et al.* showed a GaInAsP/InP single-mode semiconductor microlaser structured with a circular microcavity connected to a bus waveguide [32]. Wu *et al.* reported on unidirectional single-frequency lasing emission from a microcavity composed of a circular and a spiral rings with organic-inorganic hybrid materials [33].

Nevertheless, previous studies regarding the unidirectional and single-mode micro-lasers have been mainly performed with semiconductor and organic materials by using conventional planar photolithography technique limiting the design freedom. Therefore, three dimensional (3D) fabrication techniques allow to go one step further in optimizing towards high-efficiency single mode and uni-directional micro-laser devices. Owing to the intrinsic 3D prototyping capability with nanoscale spatial resolution, femtosecond laser processing (FLP) technique has shown to enable fabrication of a variety of micro-devices such as micro-optics, micro-mechanic and micro-fluidic devices [34]. In addition, this technique allows in situ fabrication in principle without the need for spin coating, which may be an advantage in case only single chips and not wafers are available (e.g. for prototyping). Recently, femtosecond laser direct writing of polymer microcavities with either unidirectional multi-modes or isotropic single-mode emissions was also reported recently [35], [36]. However, supporting pedestals beneath the cavities lead to difficulties in fabrication of some special types of micro structures such as ring-shaped cavity, as well as in connection of the microcavity to other optical elements. In addition, collapses

Manuscript received November 16, 2016; revised February 13, 2017 and February 15, 2017; accepted February 15, 2017. Date of publication February 16, 2017; date of current version April 20, 2017. This work was supported in part by the National Basic Research Program of China under Grant 2014CB921302, and in part by the National Natural Science Foundation of China under Grant 61427816, Grant 61235003, Grant 61625501 and Grant 61590930. *(Xue-Peng Zhan and Ying-Xin Xu contributed equally to this work.)*

X.-P. Zhan, H.-L. Xu, Q.-L. Huang, Z.-S. Hou, Q.-D. Chen, and H.-B. Sun are with the State Key Laboratory on Integrated Optoelectronics, College of Electronic Science and Engineering, Jilin University, Changchun 130012, China (e-mail: huailiang@jlu.edu.cn; hbsun@jlu.edu.cn).

Y.-X. Xu and W. Fang are with the State Key Laboratory of Modern Optical Instrumentation, College of Optical Science and Engineering, Zhejiang University, Hangzhou 310027, China (e-mail: wfang08@zju.edu.cn).

Color versions of one or more of the figures in this paper are available online at http://ieeexplore.ieee.org.

Digital Object Identifier 10.1109/JLT.2017.2671402

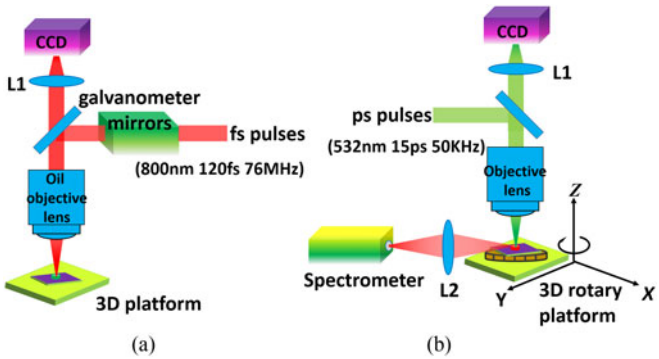

Fig. 1. Schematic diagrams of the (a) FLP and (b) optical measurement setups.

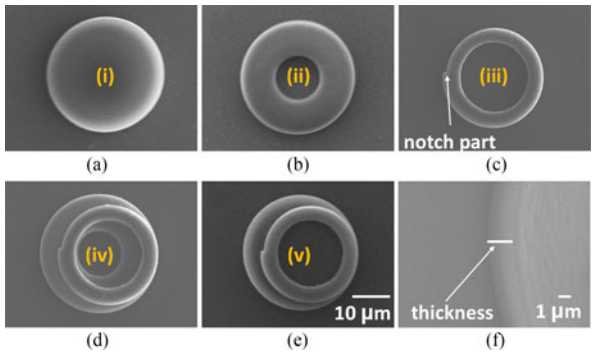

Fig. 2. (a-e) Top-view SEM micrographs for the microlasers fabricated on a NBF substrate with the shapes of (i) circular disk, (ii) circular ring, (iii) spiral ring, (iv) spiral ring stacked on circular ring, and (v) spiral ring stacked on circular disk. The diameter of the circular disk and circular ring is ~30.2 μm and the hole in the circular ring has a diameter of ~12.1 μm. The diameter of the spiral-ring is ~24.0 μm and the inner diameter of the spiral-ring is ~18.1 μm with the notch size of ~1.0 μm. (a-e) have the same scale bar of 10 μm. (f) Tilt-view magnified SEM micrograph of the circular ring in (d). The thickness of all the fabricated cavities is ~2.5 μm.

of the non-supporting microcavity edge unavoidably occur during the long-term usage of the device.

In the current study, we demonstrate, by using the FLP technique, the 3D fabrication of a polymer microlaser directly located on a 532 nm narrow band-pass filter substrate, which serves as a stable working platform. The 3D on-chip microlaser is composed of two stacked microcavities with circular-ring and spiral-ring shapes, which produces a unidirectional and single-mode output with a lasing threshold of 60 μ J/cm^2 at room temperature. We verify that a coupling occurs between the stacked microcavities by comparing lasing spectra and thresholds of different shapes of microcavities, and find that the circular-ring-shaped microcavity works as an oscillator, and the spiral-ring-shaped microcavity serves as a mode selector and a launch port. The realization of the functional coupled polymer microlasers without supporting pedestals provides a step towards the fabrication of organic integrated photonic devices by the FLP technique.

II. Experiments

The schematic diagram of the experimental FLP setup is shown in Fig. 1(a). Pulses from a Ti:Sapphire femtosecond oscillator (Tsunami, Spectra Physics) with a central wavelength of 800 nm, a pulse width of 120 fs and a repetition rate of 76 MHz were focused into the sample (see below) by an oil-immersion objective lens (NA $=1.35$, 100x). The scattered light from the sample was collected by a lens (L1: f $=5$ cm) and sent to a CCD for monitoring the processing process. A set of two galvanometer mirrors in the laser propagation path and a piezoelectric stage under the substrate was used to control the position of the laser focal spot in the sample along the horizontal and vertical directions, respectively. The laser power before the objective lens was fixed to be 7.0 mW, controlled by a variable neutral filter, and the exposure time at each focusing spot was 1 ms.

The microlasers were fabricated by the FLP technique via two-photon polymerization of dye-doped (RhB) negative photoresist (SU-8 polymer). The viscous photoresist SU-8 (MicroChem Corp.) was mixed with laser dye (RhB, 1.4 wt%), which serves as the gain medium. The mixture was dissolved in cyclopentanone. The solution was tipped on the NBF substrate (Fushen Guangdian Comp.), which was cleaned in sequence with acetone, ethanol and deionized water. The sample on the substrate was soft-baked at 95 °C on a hot-pot for 2 hours, and then processed by femtosecond laser direct writing. After the sample was processed, it was post-baked at 95 °C for 15 minutes, and then rinsed in acetone to remove the unsolidified photoresist, and as a result the fabricated microcavities were left on the substrate. Because the scanning speed and the laser power of the femtosecond laser were fixed during the fabrication, the solidified material should have the same refractive index everywhere in the developed devices.

The morphology of the fabricated microcavities were imaged by using a scanning electron microscope (JEOL JSM-7500F), and the lasing properties of the fabricated microcavities were measured by using a home-built micro-photoluminescence (μ-PL) system (see Fig. 1(b)). A picosecond frequency-doubled 532 nm, 15 ps, 50 KHz Nd:YLF laser (Amberpico-Q-2000, Guoke) was adopted to pump the microcavities. The pump laser beam was focused on the microcavities by an objective lens (NA $=0.25$, 10x), and an electric shutter was inserted into the pump laser beam to keep the exposure time of the pump laser on the sample at 20 ms, in order to avoid the bleaching effect of laser dye molecules. The lasing spectra and the far-field intensity distributions of the microlasers were measured by a spectrometer (SR-303I-A, Andor), and a rotary stage and a 3D stage were employed to precisely control the position and the orientation of the fabricated microcavity. A CCD camera was used to monitor the pumping process in the μ-PL system. The 3D FDTD simulation was carried out using commercial FDTD Solutions software. To simplify the simulation, the cavities simulated were free suspended in air. A short pulse was first launched into the cavity, and fast Fourier transfer calculation was performed to obtain the resonant spectrum of the cavity long after the pulse ceased. The far-field intensity angular distribution was calculated by exciting single resonant mode.

III. Results and Discussion

We carried out 3D finite-difference time-domain simulation, which shows that the coupling between the stacked

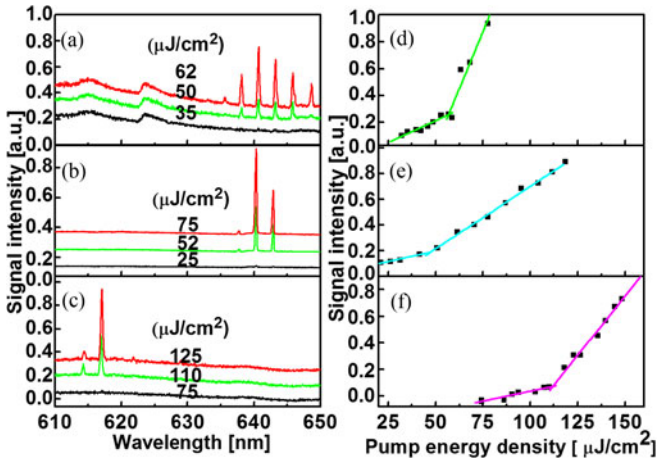

Fig. 3. (a)–(c) Room-temperature spectra of the microcavities (i-iii) obtained with three different pump laser energy densities, and (d)–(f) lasing signal intensity versus pump energy density obtained from the microlasers with (a), (d) structure (i), (b), (e) structure (ii), and (c), (f) structure (iii). All the cavities were pumped by a Nd:YLF picosecond laser with 532 nm, 15 ps, 50 kHz.

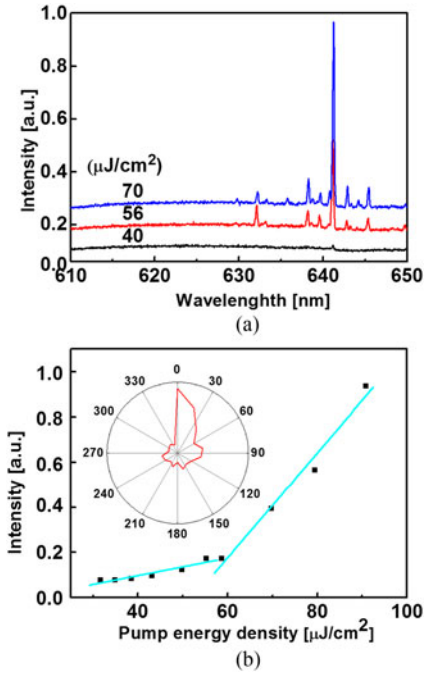

Fig. 4. (a) Room-temperature spectra of the microcavity (iv) obtained with three different pump laser energy densities, and (b) lasing threshold obtained from the microcavity (iv). Inset in (b): Far-field angular-dependent intensity distribution of the unidirectional lasing emission with a far field divergence of about 20°.

microcavities can occur, resulting in single-mode unidirectional laser output. We will introduce the simulation in details later to interpret the experimental results observed below.

In the experiments, we first fabricated several different structures of single polymer microcavities directly on a 532 nm NBF substrate with the FLP technique (for details, see Experiments). Shown in Fig. 2(a)–(c) are the top-view scanning electron microscope (SEM) micrographs for the structures of (i) circular-disk, (ii) circular-ring and (iii) spiral-ring microcavities, respectively. We refer to these three structures with labels (i), (ii) and (iii) for further discussion. Both the microcavities (i) and (ii) have an outer diameter of $\sim$30.2 μm. The inner diameter of the microcavity (ii) is $\sim$12.1 μm. The microcavity (iii) is fabricated according to the defined profile of (r, φ) as $r(\varphi) = r_0 1 + \varepsilon\varphi/(2\pi)$ in a polar coordinate with $\varepsilon = 0.083$ being the deformation parameter and $r_0 = 12$ μmt being the radius at $\varphi = 0$. As a result, the notch size is $\sim$1.0 μm. The inner diameter of the spiral ring structure (iii) is $\sim$18.1 μm. The thickness of all the fabricated microcavities is $\sim$2.5 μm, as shown in Fig. 2(f) with a magnified SEM micrograph. It is clearly shown that the fabricated microcavity is directly sitting on the substrate without a supporting pillar beneath.

In order to realize a low-threshold, unidirectional and single-mode lasing output, integrated microcavities with a spiral-ring-shaped microcavity stacked respectively on a circular-ring-shaped microcavity (Fig. 2(d)) and on a circular-disk-shaped microcavity (Fig. 2(f)) were also fabricated. For comparison, the on-chip circular- and circular-ring-shaped disks in Fig. 2(d) and (e) have the same sizes as those shown in Fig. 2(a) and (b). We refer to these two structures with labels (iv) and (v) for further discussion. In both the stacked microlasers, the on-top microcavity was designed to be tangent with the bottom microcavity to ensure efficient coupling between the top and bottom cavities. The larger circumference difference in the top and bottom cavities ensures the operation of single mode output as explained later.

With the optical measurement setup described in Experiments, we collected the emission spectra from the single microcavity from side, as shown in Fig. 3(a)–(c). The peaks appearing on the broad emission spectrum clearly indicate the occurrence of lasing actions in these single microcavities with Rhodamine B (RhB) dye as the gain medium. Multi-modes lasing from 635 nm to 650 nm oscillates within the microcavity (i), but less laser modes are observed for the microcavities (ii) and (iii). However, it should be pointed out that under the same optical excitation, no lasing action can be observed with those microcavities fabricated directly on a glass substrate (not shown). The NBF substrate prevents leakage of the optical emissions into the substrate in the spectral range of laser dye, but has a high transmission for the pumping light at 532 nm to avoid the possible interaction of the pump laser with the substrate surface as well the influence on the fabricated microcavities.

We also measured the laser intensity as a function of the pump energy density for the three microcavities (i-iii), in order to examine the lasing thresholds of different microcavities. As shown in Fig. 3(d)–(f), the measured data (solid rectangles) for the spectral modes of the three microcavities (i-iii) at 640.7, 640.5, and 617.1 nm can be well fitted by two linear curves (solid lines), from which the lasing thresholds are determined to be $\sim$57, 47 and 110 μJ/cm^2. Other modes in Fig. 3(a) and (b) show similar input-output characteristics. It can also be seen from Fig. 3(c) that the spiral-ring-shaped microcavity shows a single-mode laser output due to the small mode volume, but the lasing threshold (110 μJ/cm^2) of this microlaser is much larger than the circular (57 μJ/cm^2) and circular-ring (47 μJ/cm^2) shaped WGM ones.

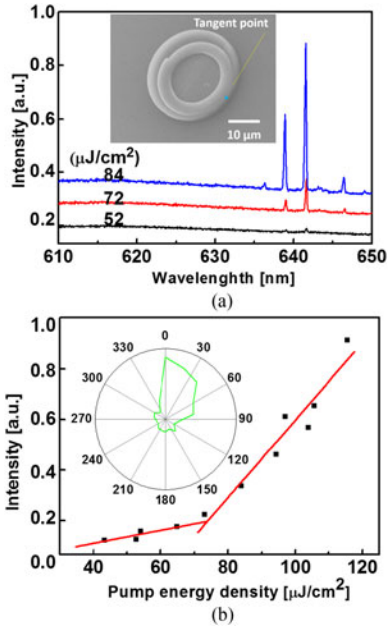

Fig. 5. (a) Room-temperature spectra of the microcavity (v) obtained with three different pump laser energy densities. Inset in (a): SEM micrograph of the tilted microlaser shows the tangent point of the two spiral and circular shaped disks. (b) Lasing threshold obtained from the microlaser (v). Inset in (b): Far-field angular-dependent intensity distribution of the lasing emission.

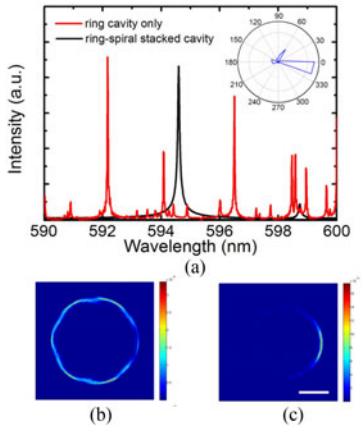

Fig. 6. (a) FDTD simulation results. The red curve and black curve represent the spectra of electromagnetic field resulted from a ring cavity and a cavity with spiral ring stacked on circular ring, respectively. The inset illustrates the far-field intensity angular distribution of the mode at 594.6 nm from the stacked cavity. (b) and (c) are the mode intensity distributions in underneath circular-ring cavity and the top spiral-ring cavity, respectively. The scale bar is 5 μm.

The emission spectra of the stacked polymer microlasers with the structures (iv and v) were also measured. A strong lasing peak at the wavelength of ~641.1 nm surrounding with suppressed small peaks can be clearly seen in Fig. 4(a) for the structure (iv) showing the single-mode laser output can be achieved by this microlaser. The reproducibility of single-mode lasing output from such microcavities was verified by fabricating different samples and observing their lasing spectra. The lasing intensity measured as a function of the pump energy density at room temperature is shown in Fig. 4(b), giving a lasing threshold of ~60 μJ/cm^2. This result agrees well with the one (48 μ J/cm^2) reported for a planer ring-spiral microlaser [33]. We also measured the angular dependence of the single-mode emission, as plotted in a polar coordinate in the inset of Fig. 4(b), from which it can been seen that the stacked microlaser exhibits a good unidirectional radiation emitted from the notch with a far field divergence of about 20° (Note that the zero degree refers to the direction facing the notch section of the on-top spiral-shaped microcavity).

It can be noted that the lasing threshold of the microlaser is comparable to those obtained from the single circular or circular-ring microlasers, but about half as that obtained from the single spiral-ring microlaser. It can also be seen that the unidirectional emission shown in the inset of Fig. 4(b) has the same feature as that of the spiral-shaped microcavity [36], However, the laser mode wavelength shown in Fig. 4(a) is totally different from the single spiral-shaped microcavity (see Fig. 3(c)), but in the lasing spectral range of the circular disk or circular ring on the long wavelength side (see Fig. 3(a) and (b)). Therefore, most likely, the on-chip circular-ring-shaped microcavity works as an oscillator that provides the WGM lasing emissions with a low lasing threshold, and then the laser modes are coupled to the on-top spiral-ring-shaped microcavity that serves as a mode selector and a launch port to emit the single-mode unidirectional radiation from the notch. In this case, small cavity volume of the oscillator is critical to realize single mode output.

In Fig. 5(a), the emission spectrum of the stacked microcavity (v) is demonstrated, from which multiple peaks can be observed. The measurement of the lasing threshold for the 641.0-nm laser mode at room temperature (Fig. 5(b)) gives a value of ~72 μ J/cm^2. The other laser mode at 639.0 nm shows a similar input-output characteristic, resulting in a lasing threshold of ~68 μ J/cm^2. The angular dependence measurement is presented in the inset of Fig. 5(b), and the far-field intensity distribution of the lasing mode at 641.6 nm also exhibits a unidirectional emission property.

Since the microcavity (i) can produce more lasing modes (see Fig. 3(a) and (b)). Therefore, it is possible for the microlaser (v) to generate a multiple-modes laser output if the on-top mode selector couldn't filter out all the other modes. As expected, it can be seen in Fig. 5(a) that double peaks appear. In addition, the far-field angular intensity distribution (Fig. 5(b)) shows very similar pattern as the one shown in Fig. 4(b). This may indicate the directionality of the laser output mainly depending on the property of the on-top spiral-ring-shaped microcavity. That is, the on-chip circular-shaped microcavity generates the lasing modes that are coupled to the on-top spiral-ring-shaped microcavity to produce unidirectional radiation from the notch.

To verify the coupling, in the 3D FDTD simulations we duplicated the structures in our simulation, but proportionally shrunk the dimension of the cavity to half in the simulation due to limited computational power. Though the chaotic nature of the stacked cavities makes tracking certain optical modes and investigating how they evolve with thickness or relative displacement very difficult, especially for large cavities, the simulation results successfully mimic our experimental ones. As shown in Fig. 6(a), for a ring cavity, multiple sharp peaks can be found

in the spectral range from 590 nm to 600 nm, which indicates the existence of many high-Q modes. However, when a spiral-shaped cavity was placed on the top of the ring cavity, the breaking of rotational symmetry destroyed most high-Q WGMs, and only one high peak at 594.6 nm can be seen within this wavelength range. Far-field intensity angular distribution was also calculated for this high-Q mode and plotted as inset in Fig. 6(a), which illustrated single directional output. The mode intensity distributions of the plans in circular-ring cavity (Fig. 6(b)) and in spiral-ring cavity (Fig. 6(c)) validate our hypothesis. The intensity profile in circular-ring microcavity shows WGM like shape, indicating a high-Q mode at 594.6 nm; while the strong asymmetry distribution in spiral-ring cavity disclose the non-resonance at 594.6 nm. Generally, in such case, the energy coupled from circular-ring cavity to the spiral-ring cavity will dissipate due to the boundary scattering, so that high-Q properties of WGMs in circular-ring microcavity cannot be maintained. However, in some circumstance, as shown in Fig. 6(c), the light may couple back to the circular-ring cavity along the circumference, with very small proportion emitted directionally at the notch region. Thus the mode quality is preserved, and single directional output is achieved. Though the simulated structure is not exactly the same as experimental one, these results clearly demonstrate the high possibility of single-mode lasing with unidirectional output from such stacked cavity, which helps the interpretation of the cavity emission performance observed in Figs. 3–5.

Based on the WGMs theory, the free spectral range (FSR) can be estimated based on the relation $\Delta\lambda = \lambda^2/(n\pi d)$ with λ being the emission wavelength, n being the refractive index and d being the diameter. Thus, the FSR of the microlasers with the structures (i) and (ii) is calculated to be $\sim$2.55 nm at the wavelength of 640.7 nm with the effective refractive index [35]. This agrees well with the measured FSRs for the microcavities (i) ($\sim$2.52 nm) and (ii) ($\sim$2.55 nm), showing the WGMs features of these two microcavities. It can also be seen from Fig. 3(a) and (b) that as the volume decreases, the number of the WGMs is significantly reduced, providing a way to produce single-mode laser output. However, the rotational symmetry of the WGMs microlasers results in isotropic emissions in both the near and far fields.

We calculated the Q factors according to the relation of $Q = \nu/\delta\nu$, where $\nu = c/\lambda$ is the frequency of the lasing emission and $\delta\nu$ is the full width at half maximum (FWHM) of the lasing line frequency, respectively. Since the measured linewidths result from the stimulated emission of the active microcavities, the Q factors might be overestimated due to the spectral narrowing effect. Therefore, the linewidths measured with the pump powers right below the lasing threshold were used for estimating the Q-factors, in order to minimize the effect of spectral narrowing. As a result, the measured spectral linewidths for the microcavities (i-v) are 0.29, 0.28, 0.34, 0.28, and 0.29, respectively. We also consider the instrumental broadening effect of the spectrometer. Since the linewidth of a HeNe laser is typically 1 GHz or less, we measured the spectral line of the HeNe laser at 632 nm, which gives a value of 0.28 nm. Therefore, the instrumental broadening is determined to be $\sim$0.27 nm. That is, the measured profile of the HeNe laser line reflects the instrumental broadening of the spectrometer. By deconvoluting the experimental curves with the instrumental broadening profile, the Q values are estimated to be $\sim 6.2 \times 10^3$, 6.0×10^3, 4.6×10^3, 6.1×10^3, and 7.3×10^3, respectively. In Table I, we list the measured Q values and lasing thresholds of the microcavities (i-v). The relative large laser threshold for the structure (iii) may result from the relatively low Q factor of this microcavity when compared with those of the microlasers (i and ii).

TABLE I
LASING MODE AND CORRESPONDING Q VALUES AND THRESHOLDS FOR THE MICROCAVITIES WITH THE FIVE STRUCTURES

Structure	Lasing mode	Q value	Lasing threshold
(i)	640.7 nm	6.2×10^3	57 μJ/cm^2
(ii)	640.5 nm	6.0×10^3	47 μJ/cm^2
(iii)	617.1 nm	4.6×10^3	110 μJ/cm^2
(iv)	641.6 nm	6.1×10^3	72 μJ/cm^2
(v)	641.1 nm	7.3×10^3	60 μJ/cm^2

(i): Circle disk; (ii): circle ring; (iii): spiral ring; (iv): spiral ring stacked on the circle ring; (v): spiral ring stacked on the circle disk.

IV. CONCLUSION

In summary, we have fabricated a 3D on-chip coupled polymer microlaser by the FLP technique via two-photon polymerization, and demonstrated that the microlaser enables operation of unidirectional and single-mode laser output with a low lasing threshold at room temperature. The coupling between the on-chip circular-ring microcavity and on-top spiral-ring microcavity in the microlaser was verified by comparing the laser spectra, lasing thresholds, and Q factors of a variety of different structured microlasers. It was found that the circular-ring microcavity serves as an oscillator to provide the low-threshold WGMs lasing emissions, and the spiral-ring microcavity works as a mode filter and output port. The demonstration of the functional integrated polymer microlasers fabricated by the FLP technique provides an important step towards integrated organic photonic microdevices. However, it is clear that much additional effort is needed for practical applications of these devices, such as integrating these devices with optical waveguides and other components, and developing certain compact and inexpensive diode lasers for pumping source.

REFERENCES

[1] T. J. Kippenberg and K. J. Vahala, "Cavity opto-mechanics," *Opt. Express*, vol. 15, no. 25, pp. 17172–17205, Dec. 2007.
[2] M. Metcalfe, "Applications of cavity opto-mechanics," *Appl. Phys. Rev.*, vol. 1, no. 3, pp. 1–18, Sep. 2014, Art. no. 031105.
[3] K. H. Kim *et al.*, "Cavity optomechanics on a microfluidic resonator with water and viscous liquids," *Light-Sci. Appl.*, vol. 2, no. 11, pp. 1–5, Nov. 2013, Art. no. e110.
[4] Y. S. Park, A. K. Cook, and H. Wang, "Cavity QED with diamond nanocrystals and silica microspheres," *Nano Lett.*, vol. 6, no. 9, pp. 2075–2079, Aug. 2006.
[5] S. M. Spillane, T. J. Kippenberg, K. J. Vahala, K. W. Goh, E. Wilcut, and H. J. Kimble, "Ultrahigh-Q toroidal microresonators for cavity quantum electrodynamics," *Phys. Rev. A.*, vol. 71, no. 1, pp. 1–10, Jan. 2005, Art. no. 013817.
[6] Y. Wu, "Quantum theory of microcavity-modified fluorescence decay rate under a strong coupling condition," *Phys. Rev. A*, vol. 61, no. 3, pp. 1–6, Feb. 2000, Art. no. 033803.

[7] Y. Wu and X. Yang, "Quantum theory for microcavity enhancement of second harmonic generation," *J. Phys. B, Atomic, Mol. Opt. Phys.*, vol. 34, no. 11, pp. 2281–2288, Apr. 2001.
[8] P. Rabiei, W. H. Steier, C. Zhang, and L. R. Dalton, "Polymer microring filters and modulators," *IEEE. J. Lightw. Technol.*, vol. 20, no. 11, pp. 1968–1975, Nov. 2002.
[9] P. D. Batista, B. Drescher, W. Seidel, J. Rudolph, S. Jiao, and P. V. Santos, "ZnO/SiO_2 microcavity modulator on silicon," *Appl. Phys. Lett.*, vol. 92, no. 13, pp. 1–3, Apr. 2008, Art. no. 133502.
[10] V. S. Ilchenko and A. B. Matsko, "Optical resonators with whispering-gallery-modes part II: Applications," *IEEE J. Sel. Topics Quantum Electron.*, vol. 12, no. 1, pp. 15–32, Feb. 2006.
[11] M. K. Chin *et al.*, "GaAs microcavity channel-dropping filter based on a race-track resonator," *IEEE Photon. Technol. Lett.*, vol. 11, no. 12, pp. 1620–1622, Dec. 1999.
[12] E. Krioukov, D. J. W. Klunder, A. Driessen, J. Greve, and C. Otto, "Sensor based on an integrated optical microcavity," *Opt. Lett.*, vol. 27, no. 7, pp. 512–514, Apr. 2002.
[13] S. Mehrabani, P. Kwong, M. Gupta, and A. M. Armani, "Hybrid microcavity humidity sensor," *Appl. Phys. Lett.*, vol. 102, no. 24, pp. 1–4, Jun. 2013, Art. no. 241101.
[14] J. F. Ku, Q. D. Chen, R. Zhang, and H. B. Sun, "Whispering-gallery-mode microdisk lasers produced by femtosecond laser direct writing," *Opt. Lett.*, vol. 36, no. 15, pp. 2871–2873, Aug. 2011.
[15] Y. Wu and P. T. Leung, "Lasing threshold for whispering-gallery-mode microsphere lasers," *Phys. Rev. A*, vol. 60, no. 1, pp. 630–633, Jul. 1999.
[16] A. M. Flatae *et al.*, "Optically controlled elastic microcavities," *Light-Sci. Appl.*, vol. 4, pp. 1–5, Apr. 2015, Art. no. e282.
[17] S. Y. Lu *et al.*, "Highly stable on-chip embedded organic whispering gallery mode lasers," *IEEE J. Lightw. Technol.*, vol. 32, no. 13, pp. 2415–2419, Jul. 2014.
[18] D. E. Gomez, I. Pastoriza-Santos, and P. Mulvaney, "Tunable whispering gallery quantum-dot-doped mode emission from microspheres," *Small*, vol. 1, no. 2, pp. 238–241, Feb. 2005.
[19] T. Harayama and S. Shinohara, "Two-dimensional microcavity lasers," *Laser Photon. Rev.*, vol. 5, no. 2, pp. 247–271, Mar. 2011.
[20] J. Wiersig and M. Hentschel, "Unidirectional light emission from high-Q modes in optical microcavities," *Phys. Rev. A.*, vol. 73, no. 3, pp. 1–4, Mar. 2006, Art. no. 031802(R).
[21] S. Lacey and H. Wang, "Directional emission from whispering-gallery modes in deformed fused-silica microspheres," *Opt. Lett.*, vol. 26, no. 24, pp. 1943–1945, Dec. 2001.
[22] C. Gmachl *et al*., "High-power directional emission from microlasers with chaotic resonators," *Science*, vol. 280, no. 5369, pp. 1556–1564, Jun. 1998.
[23] S. Chang, R. K. Chang, A. D. Stone, and J. U. Nöckel, "Observation of emission from chaotic lasing modes in deformed microspheres: displacement by the stable-orbit modes," *J. Opt. Soc. Amer. B*, vol. 17, no. 11, pp. 1828–1834, Nov. 2000, Art. no. 031802(R).
[24] S. K. Kim, S. H. Kim, G. H. Kim, H. G. Park, D. J. Shin, and Y. H. Lee,"Highly directional emission from few-micron-size elliptical microdisks," *Appl. Phys. Lett.*, vol. 84, no. 6, pp. 861–863, Feb. 2004.
[25] S. Juodkazis, K. Fujiwara, T. Takahashi, S. Matsuo, and H. Misawa, "Morphology-dependent resonant laser emission of dye-doped ellipsoidal microcavity," *J. Appl. Phys.*, vol. 91, no. 3, pp. 916–921, Feb. 2002.
[26] G. D. Chern, H. E. Tureci, A. D. Stone, R. K. Chang, M. Kneissl, and N. M. Johnson, "Unidirectional lasing from InGaN multiple-quantum-well spiral-shaped micropillars," *Appl. Phys. Lett.*, vol. 83, no. 9, pp. 1710–1712, Sep. 2003.
[27] T. Ben-Messaoud and J. Zyss, "Unidirectional laser emission from polymer-based spiral microdisks," *Appl. Phys. Lett.*, vol. 86, no. 24, pp. 1–3, Jun. 2005, Art. no. 241110.
[28] R. Chen and H. D. Sun, "Single mode lasing from hybrid hemispherical microresonators," *Sci. Rep.*, vol. 2, no. 244, pp. 1–6, Feb. 2012.
[29] L. Shang, L. Liu, and L. Xu, "Single-frequency coupled asymmetric microcavity laser," *Opt. Lett.*, vol. 33, no. 10, pp. 1250–1152, May 2008.
[30] V. D. Ta, R. Chen, and H. Sun, "Coupled polymer microfiber lasers for single mode operation and enhanced refractive index sensing," *Adv. Opt. Mater.*, vol. 2, no. 3, pp. 220–225, Mar. 2014.
[31] S. Yang, Y. Wang, and H. Sun, "Advances and prospects for whispering gallery mode microcavities," *Adv. Opt. Mater.*, vol. 3, no. 9, pp. 1136–1162, Sep. 2015.
[32] Y. Z. Huang *et al.*, "Unidirectional-emission single mode whispering-gallery-mode microlasers," *Proc. SPIE*, vol. 8236, pp. 1–8, Jan. 2012, Art. no. 82360M.
[33] X. Wu, H. Li, L. Liu, and L. Xu, "Unidirectional single-frequency lasing from a ring-spiral coupled microcavity laser," *Appl. Phys. Lett*, vol. 93, no. 8, pp. 1–3, Aug. 2008, Art. no. 081105.
[34] Y. L. Zhang, Q. D. Chen, H. Xia, and H. B. Sun, "Designable 3D nanofabrication by femtosecond laser direct writing," *Nano Today*, vol. 5, no. 5, pp. 435–448, Sep. 2010.
[35] J. F. Ku *et al.*, "Photonic-molecule single-mode laser," *IEEE Photon. Technol. Lett.*, vol. 27, no. 11, pp. 1157–1160, Jun. 2015.
[36] X. P. Zhan *et al.*, "Unidirectional lasing from a spiral-shaped microcavity of dye-doped polymers," *IEEE Photon. Technol. Lett.*, vol. 27, no. 3, pp. 311–314, Jan. 2015.

Xue-Peng Zhan received the B.S. degree in 2012 from the College of Electronic Science and Engineering, Jilin University, Changchun, China, where he is currently working toward the Ph.D. degree. His research interests include femtosecond laser fabrication of integrated organic optoelectronic devices.

Ying-Xin Xu received the B.S. degree in 2012 from the Department of Optical Engineering, Zhejiang University, Hangzhou, China, where he is currently working toward the Ph.D. degree. His research interests include micro/nanofiber fabrication and applications.

Huai-Liang Xu received the Ph.D. degree in physics from Lund University, Lund, Sweden, in 2004. He was a Postdoctoral Researcher with the Laval University of Canada. In January 2008, he became an Assistant Professor at the University of Tokyo, Tokyo, Japan. Since September 2009, he has been a Full Professor at Jilin University, Changchun, China. His research interests include ultrafast strong laser sensing, strong-field laser physics, and atomic and molecular spectroscopy.

Qiu-Lan Huang received the B.S. degree in 2013 from the College of Electronic Science and Engineering, Jilin University, Changchun, China, where she is currently working toward the Ph.D. degree. Her research interests include integrated optoelectronic devices and photonic quantum devices.

Zhi-Shan Hou received the B.S. degree in 2013 from the College of Physics, Jilin University, Changchun, China, where he is currently working toward the Ph.D. degree. His research interests including the quantum chip and integrated optoelectronic devices.

Wei Fang received the Ph.D. degree in physics from the Northwestern University, Evanston, IL, USA, in 2006. He was a Postdoctoral Researcher with the National Institute of Standards and Technology. In January 2009, he became an Associate Professor at Zhejiang University. His research interests include quantum light sources and nonlinear optics in microcavities and waveguides.

Qi-Dai Chen received the Ph.D. degree in plasma physics from the Institute of Physics, Chinese Academy of Sciences, Beijing, China, in 2004. He was a JST Postdoctoral Researcher at Osaka City University of Japan. In 2006, he was employed as an Associate Professor in the College of Electronic Science and Engineering, Jilin University. In 2011, he was promoted as a Full Professor. His research interests include laser nanofabrication technology for microoptics, semiconductor laser beam shaping, and subwavelength antireflective microstructure.

Hong-Bo Sun received the Ph.D. degree in electronics from Jilin University, Changchun, China, in 1996. He was a Postdoctoral Researcher with the University of Tokushima, from 1996 to 2000, and an Assistant Professor at Osaka University. In 2005, he was promoted as a Full Professor (Changjiang Scholar) in Jilin University. He received the Outstanding Young Scientist Award issued by the minister of MEXT (Japan) in 2006. His research interests include laser nanofabrication and ultrafast spectroscopy.